Witold M. Bloch, Christian J. Doonan and Christopher J. Sumby
Using hinged ligands to target structurally flexible copper(II) MOFs
Crystengcomm, 2013; 15(45):9663-9671

Published at: http://dx.doi.org/10.1039/C3CE41244J

Journal Name

Dynamic Article Links►

Cite this: DOI: 10.1039/c0xx00000x

www.rsc.org/xxxxxx

ARTICLE TYPE

Using hinged ligands to target structurally flexible copper(II) MOFs

Witold M. Bloch,[a] Christian J. Doonan[a] and Christopher J. Sumby[a]*

Received (in XXX, XXX) XthXXXXXXXXX 20XX, Accepted Xth XXXXXXXXX 20XX
DOI: 10.1039/b000000x

Here we report two new flexible MOFs based on a bis-pyrazolylmethane 'hinged' link design that favours the formation of two distinct structural nodes within the resulting 2-D and 3-D structures. The less sterically demanding ligand H_2**bcppm** affords a 2-D layered MOF, $\{Cu_2[Cu^{II}(NO_3)_2(\mathbf{bcppm})_2](DMF)_2\}\cdot 2DMF$ (**1**), constructed from copper(II) paddlewheel and mononuclear octahedral copper(II) nodes. The use of a more sterically encumbered tetramethyl analogue H_2**bcpdmpm** induces a dramatic twisting of the ligand backbone that yields a 3-D MOF$\{Cu_4[Cu^{I}(\mathbf{bcpdmpm})_2]_2(EtOH)_2(H_2O)_2\}(NO_3)_2\cdot 12DMF$ (**2**) formed from a very similar mix of nodes, specifically copper(II) paddlewheel clusters and mononuclear tetrahedrally coordinated copper(I) centres. Herein we describe the crystal structures, solid-state flexibility, and gas adsorption properties of both materials.

Introduction

Flexible metal-organic frameworks (MOFs) have attracted significant attention as their dynamic structures give rise to properties that are not accessible for rigid architectures.[1-5] Such materials, sometimes called third generation porous coordination polymers (PCPs),[6] show 'gated' adsorption behaviour that results in remarkable, pressure dependent, selective gas uptake.[7-15] In addition, structural flexibility in MOFs, has facilitated the preparation of chemical sensors,[16] and materials for controlled release of active pharmaceuticals.[17, 18]

Structural flexibility[3, 6] can be introduced into MOF materials *via* judicious choice of metal nodes,[5, 19] non-rigid organic links,[11, 13] or by utilising weak non-covalent interactions between two or more interpenetrated frameworks.[20] As part of our investigations into flexible solid-state materials, we reported the synthesis of a flexible material comprised of silver(I) and a di-2-pyrazinylmethane (**dpzm**, Figure 1) organic building block.[21] This organic moiety possesses a methylene 'hinge' between two pyrazine donors where one nitrogen donor from each pyrazine ring can chelate a single metal while the other two donors can coordinate to two further metal centres. Significantly, the relative positions of the two bridging donor nitrogen atoms can be controlled through changes in the coordination geometry of the chelated metal. The reported 3-D PCP undergoes crystal-to-crystal breathing upon solvent exchange and, in the case of the particular example reported, a 3-D to 2-D structural change.[21] Building on our earlier work, we have extended the hinged link approach to ligands capable of providing more chemically and thermally stable MOFs. Reaction of **bcppm** (Figure 1) with $Cu(NO_3)_2$ yielded the extended network $[Cu(\mathbf{bcppm})H_2O]$.[22] Heating the as-synthesised material under vacuum generated a locked and pore constricted version of the framework that displayed exceptional CO_2/N_2 selectivity. We note that this is a rare example of utilising symmetrical bis-pyrazolylmethane building blocks in the synthesis of extended network materials.[23, 24]

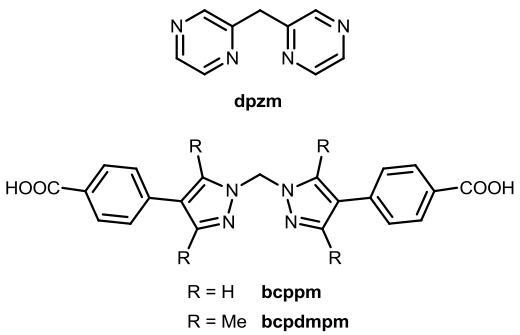

Figure 1. Ligands possessing a methylene spacer, including the first generation 'hinged' link di(2-pyrazinyl)methane (**dpzm**) and the second generation examples bis(4-(4-carboxyphenyl)-1*H*-pyrazolyl)methane (H_2**bcppm**) and bis(4-carboxyphenyl)-3,5-dimethyl-1*H*-pyrazolyl)methane (H_2**bcpdmpm**).

In this manuscript we report two new flexible MOFs based on a bis-pyrazolylmethane 'hinged' link design that allows the incorporation of two distinct copper nodes within their 2-D and 3-D structures. The less sterically demanding ligand H_2**bcppm** affords a 2-D MOF with staggered layers, $\{Cu_2[Cu^{II}(NO_3)_2(\mathbf{bcppm})_2](DMF)_2\}\cdot 2DMF$ (**1**), while, the more sterically encumbered tetramethyl analogue H_2**bcpdmpm** yields a self-penetrating 3-D MOF, $\{Cu_4[Cu^{I}(\mathbf{bcpdmpm})_2]_2(EtOH)_2(H_2O)_2\}(NO_3)_2\cdot 12DMF$ (**2**). The structures, solid-state flexibility, and gas adsorption properties of both materials are reported.

Experimental

General Experimental

Elemental analyses were performed by the Campbell Microanalytical Laboratory at the University of Otago. Thermogravimetric analysis was performed on a Perkin−Elmer STA-6000 under a constant flow of N_2 at a temperature increase rate of 10°C/min. Infrared (IR) spectra were recorded on a Perkin−Elmer Fourier−Transform Infrared (FT−IR) spectrometer on a zinc−selenide crystal. NMR spectra were recorded on a Varian 600 MHz spectrometer at 23°C using a 5 mm probe. Unless otherwise stated, all chemicals were obtained from commercial sources and used as received. The compounds bis(4-(4-carboxyphenyl)-1*H*-pyrazolyl)methane (H_2**bcppm**)[22] and bis(3,5-dimethyl-4-iodo-1*H*-pyrazol-1-yl)methane (**3**)[25] were prepared by reported procedures.

Synthesis

Bis(4-(4-carboxyphenyl)-3,5-dimethyl-1*H*-pyrazolyl)methane (H_2bcpdmpm). Compound **3** (1.50 g, 3.29 mmol), 4-carboxyphenylboronic acid (1.64 g, 9.88 mmol) and aqueous K_2CO_3 (6.60 g, 38 mL distilled water) were combined in DMF (180 mL). After degassing the mixture with Ar for 30 minutes, $Pd(PPh_3)_4$ (0.57 g, 0.49 mmol, 0.15 equiv.) was added. The resulting mixture was further degassed for 30 minutes and then heated at 90°C for 20 hours. Upon cooling to room temperature, distilled water (200 mL) was added and the reaction mixture filtered. The resulting solution was washed with dichloromethane (5 x 50 mL) and then acidified with 20% HNO_3 (pH = 3) to afford a precipitate which was isolated under reduced pressure. The resulting white solid was washed with distilled water, ethanol and dried at 130°C to afforded H_2**bcpdmpm** (1.12 g, 76%). Mp: 281-282°C; Found C 67.5, H 5.5, N 12.7, $C_{25}H_{24}N_4O_4$ requires: C 67.6, H 5.4, N 12.6%. ν_{max} (neat, cm^{-1}): 1687 (C=O), 1608 (C=N), 1550 (C=C), 1478 (C=C). ^{1}H NMR (600 MHz/DMSO): δ 2.13 (s, 6H, CH_3), 2.47 (s, 6H, CH_3), 6.27 (s, 2H, CH_2), 7.39 (d, 4H, H2´/H6´), 7.97 (d, 4H, H3´/H5´), 12.87 (s, br, 2H, CO_2H); (150 MHz/DMSO): δ 10.1, 12.6, 59.5, 118.2, 128.4, 129.0, 129.5, 137.6, 137.9, 145.6, 167.1; *m/z* 444.9 (MH+).

{$Cu_2[Cu^{II}(NO_3)_2$(bcppm)$_2$](DMF)$_2$}·2DMF (1). In a 20 mL screw cap vial, $Cu(NO_3)_2·2½H_2O$ (27.3 mg, 0.12 mmol) was combined with H_2**bcppm** (29.5 mg, 0.08 mmol) and dissolved in a mixture of DMF (3 mL), ethanol (1 mL) and 4 drops of 70% HNO_3. The resulting mixture was heated at 85°C for 16 hours, giving crystalline powder. The crystals were washed in DMF (× 3), methanol (× 8), and dichloromethane (× 8), after which they were dried under N_2 flow, and heated at 50°C under vacuum overnight (28.2 mg, 65%, based on analysis for $\{Cu_2[Cu^{II}(NO_3)_2$(**bcppm**)$_2](H_2O)_2\}·H_2O$). ν_{max} (neat, cm^{-1}): 3122 (w, C-H), 1611 (s, C=O), 1509 (w, C=C), 1371 (s O-NO), 1301 (s, O-NO). Found C 43.44, H 3.0, N 12.1, $C_{42}H_{34}N_{10}O_{17}Cu_3$ requires C 44.2, H 3.0, N 12.3%. Crystals suitable for X-ray crystallography were grown from a mixture of DMF (1.5 mL), EtOH (1 mL) and AcOH (2 drops).

{$Cu_4[Cu^I$(bcpdmpm)$_2]_2$(EtOH)$_2$(H$_2$O)$_2$}(NO$_3$)$_2$·12DMF (2). In a 20 mL screw cap vial, $Cu(NO_3)_2·2½H_2O$ (25.5 mg, 0.11 mmol) was combined with H_2**bcpdmpm** (20.1 mg, 0.05 mmol) and dissolved in a mixture of DMF (4 mL), distilled water (0.8 mL), ethanol (1.6 mL) and 2 drops of 70% HNO_3. The resulting mixture was heated at 85°C for 16 hours, giving teal rod-like crystals suitable for X-ray crystallography. The crystals were washed with methanol (× 8) followed by dichloromethane (× 8), after which they were dried under N_2 flow, and heated at 50°C under vacuum overnight (17.0 mg, 63% based on analysis for $\{Cu_4[Cu^I$(**bcpdmpm**)$_2]_2(H_2O)_4\}(NO_3)_2·2H_2O$). Found C 50.0, H 4.4, N 10.4. $C_{100}H_{108}N_{18}O_{28}Cu_6$ requires: C 50.3, H 4.4, N 10.6%. ν_{max} (neat, cm^{-1}): 1610 (m, C=O), 1584 (m, C=C), 1509 (w, C=C), 1400 (s, O-NO), 1301 (s, O-NO).

X-ray Crystallography

Single crystals were mounted in paratone-N oil on a plastic loop. X-ray diffraction data were collected at 150(2) K on the MX1 beamline of the Australian Synchrotron (λ = 0.7107 Å). Data sets were corrected for absorption using a multi-scan method, and structures were solved by direct methods using SHELXS-97[26] and refined by full-matrix least squares on F^2 by SHELXL-97,[27]interfaced through the program X-Seed.[28] In general, all non-hydrogen atoms were refined anisotropically and hydrogen atoms were included as invariants at geometrically estimated positions, unless specified otherwise in additional details below. Figures were produced using the program CrystalMaker. CCDC 945926 and 945927 contain the supplementary crystallographic data for these structures. These data can be obtained free of charge from The Cambridge Crystallographic Data Centre via www.ccdc.cam.ac.uk/data_request/cif.

*Special Refinement Details for **1***. Two of the nitrate anions (on special positions) were refined with isotropic displacement parameters and eight DFIX restraints were used to force chemically sensible bond lengths for these anions and a DMF molecule. The structure has large solvent accessible voids. These contained a number of diffuse electron density peaks that could not be adequately identified and refined as solvent. The SQUEEZE[29] routine of PLATON was applied to the collected data, which resulted in significant reductions in R_1 and wR_2 and an improvement in the GOF. The contents of the solvent region calculated from the result of SQUEEZE routine equates to two DMF per asymmetric unit. The ADDSYM routine detects pseudo-symmetry for the structure with a low fit (81% of atom positions fulfil this symmetry element). From the structure it is clear that the different positions of the DMF ligands on the copper(II) paddlewheel units, twisting of the ligand molecules, and dissimilar coordination environments about the tetrahedral copper(I) centres, which are all a consequence of layer-layer steric constraints, break this additional symmetry element.

*Special Refinement Details for **2***.The carbon atoms of the two coordinated ethanol molecules were refined with isotropic displacement parameters and two DFIX restrains were used to achieve chemically sensible C-O bond lengths. The structure has very large solvent accessible voids. These contained a number of diffuse electron density peaks that could not be adequately identified and refined as solvent. The SQUEEZE[29] routine of PLATON was applied to the collected data, which resulted in significant reductions in R_1 and wR_2 and an improvement in the GOF. The contents of the solvent region calculated from the result of the SQUEEZE routine equates to two nitrate anions and 12 DMF molecules per asymmetric unit.

Powder Diffraction

Powder X-ray diffraction data for **1** was collected on a Rigaku Hiflux Homelab system using Cu-Kα radiation with an R-Axis IV++ image plate detector. Samples were mounted on plastic loops using paratone-N and data collected by scanning 90° in phi for 120-300 second exposures. The data was converted into xye format using the program DataSqueeze. PXRD data for **2** was collected at the Australian Synchrotron on the Powder Diffraction (PD) beamline. The sample was prepared in a glass capillary (0.3 mm) and exposed to X-rays with a wavelength of 0.82544 Å. For further details on the instrument set-up see www.synchrotron.org.au. Simulated powder X-ray diffraction patterns were generated from the single crystal data using Mercury 2.4.

Table 1. Crystal and X-ray experimental data for **1** and **2**.

Compound	**1**	**2**
Empirical formula	$C_{54}H_{56}Cu_3N_{14}O_{18}$	$C_{140}H_{188}Cu_6N_{30}O_{38}$
Formula weight	1379.75	3280.44
Crystal system	orthorhombic	monoclinic
Space group	*Pnma*	$P2_1/c$
a (Å)	15.219(3)	19.4251(9)
b (Å)	75.540(15)	36.589(2)
c (Å)	14.401(3)	37.762(2)
β (°)		114.202(4)
Volume (Å^3)	16556(6)	24480(2)
Z	8	4
D_{calc} (Mg/m^3)	1.107	0.890
Absorption coefficient (mm^{-1})	0.824	0.566
F(000)	5672	6864
Crystal size (mm^3)	0.11 x 0.06 x 0.05	0.42 x 0.10 x 0.03
Theta range for data (°)	0.54 - 27.65	0.81 - 25.99
Reflections collected	245027	348647
Independent reflections [R(int)]	19174 [0.0823]	47801 [0.0578]
Completeness to theta full (%)	99.4	99.5
Observed reflections [I>2σ(I)]	15871	33947
Data / restraints / parameters	19174/8/713	47801/2/1313
Goodness-of-fit on F2	1.029	0.971
R_1 [I>2σ(I)]	0.0815	0.0573
wR_2 (all data)	0.2618	0.1746
Largest diff. peak and hole (e.Å^{-3})	1.716 & -1.306	1.077 & -0.898

Gas adsorption measurements

Gas sorption isotherm measurements were performed on an ASAP 2020 Surface Area and Pore Size Analyzer. Activation of **1** was achieved by washing in DMF (× 3), methanol (× 8), and dichloromethane (× 8), drying under N_2 flow, and heated at 50°C under vacuum overnight. Similarly, a sample of **2** was activated by being washed with methanol (× 8) followed by dichloromethane (× 8), after which it was dried under N_2 flow, and heated at 50°C under vacuum overnight. UHP grade (99.999%) N_2 and CO_2 were used for all measurements. The temperatures were maintained at 77 K (liquid nitrogen bath), 195 K (acetone-dry ice bath), 273 K (ice−water bath), or 293 K (room temperature water), respectively. CO_2 enthalpy plots were obtained from isotherms collected at 273 and 293 K.

Results and Discussion

The previously reported MOF synthesised from the H_2**bcppm** ligand, [Cu(**bcppm**)H_2O]*x*S (S = solvent),[22] required aqueous reaction conditions (25% H_2O). Excluding water from the solvent system led to the formation of a new MOF material {Cu_2[Cu^{II}(NO_3)$_2$(**bcppm**)$_2$](DMF)$_2$}·2DMF (**1**). Reacting H_2**bcppm** with $Cu(NO_3)_2$·2½H_2O in a mixture of DMF, EtOH, and a few drops of 70% HNO_3 at 85°C gave a green micro-crystalline powder of **1** in 65% yield (Figure 2, top).The chemical composition of **1** was confirmed by elemental analysis of a dried sample ($C_{42}H_{34}N_{10}O_{17}Cu_3$). Single crystals of **1** were obtained by reacting $Cu(NO_3)_2$·2½H_2O and H_2**bcppm** in a mixture of DMF, EtOH, and a few drops of acetic acid at 65°C. These crystals were not suitable for in-house X-ray sources and thus structure elucidation was achieved using synchrotron radiation.

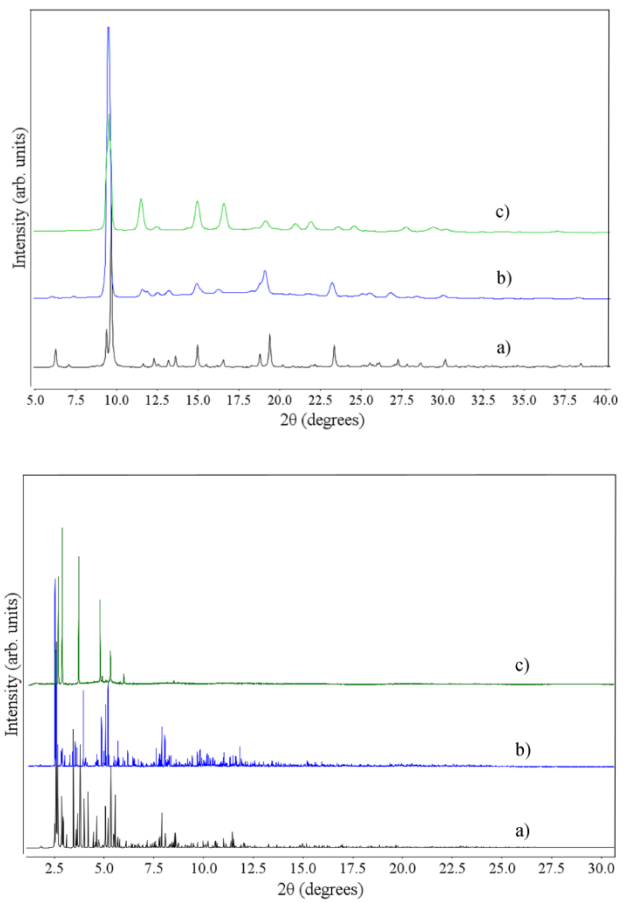

Figure 2. PXRD patterns for **1** (top): (a) simulated from the single crystal structure, (b) as synthesised, and (c) the activated material {Cu_2[Cu^{II}(NO_3)$_2$(**bcppm**)$_2$]} (**1**^{ac}).PXRD patterns for **2** (bottom): (a) simulated from the single crystal structure, (b) as synthesised, and (c) the activated material {Cu_4[Cu^{I}(**bcpdmpm**)$_2$]$_2$}(NO_3)$_2$ (**2**^{ac}).

The network topology of **1** is best described as a 2-D 4^4 net (Figure 3a) formed from **bcppm** and two distinct copper(II) nodes. Compound **1** crystallises in the orthorhombic space group *Pnma* with an asymmetric unit that contains two molecules of **bcppm**, four copper(II) centres (two on special positions), two coordinated DMF molecules and three nitrate anions (two on special positions). Two of the copper(II) centres form a dimetallic

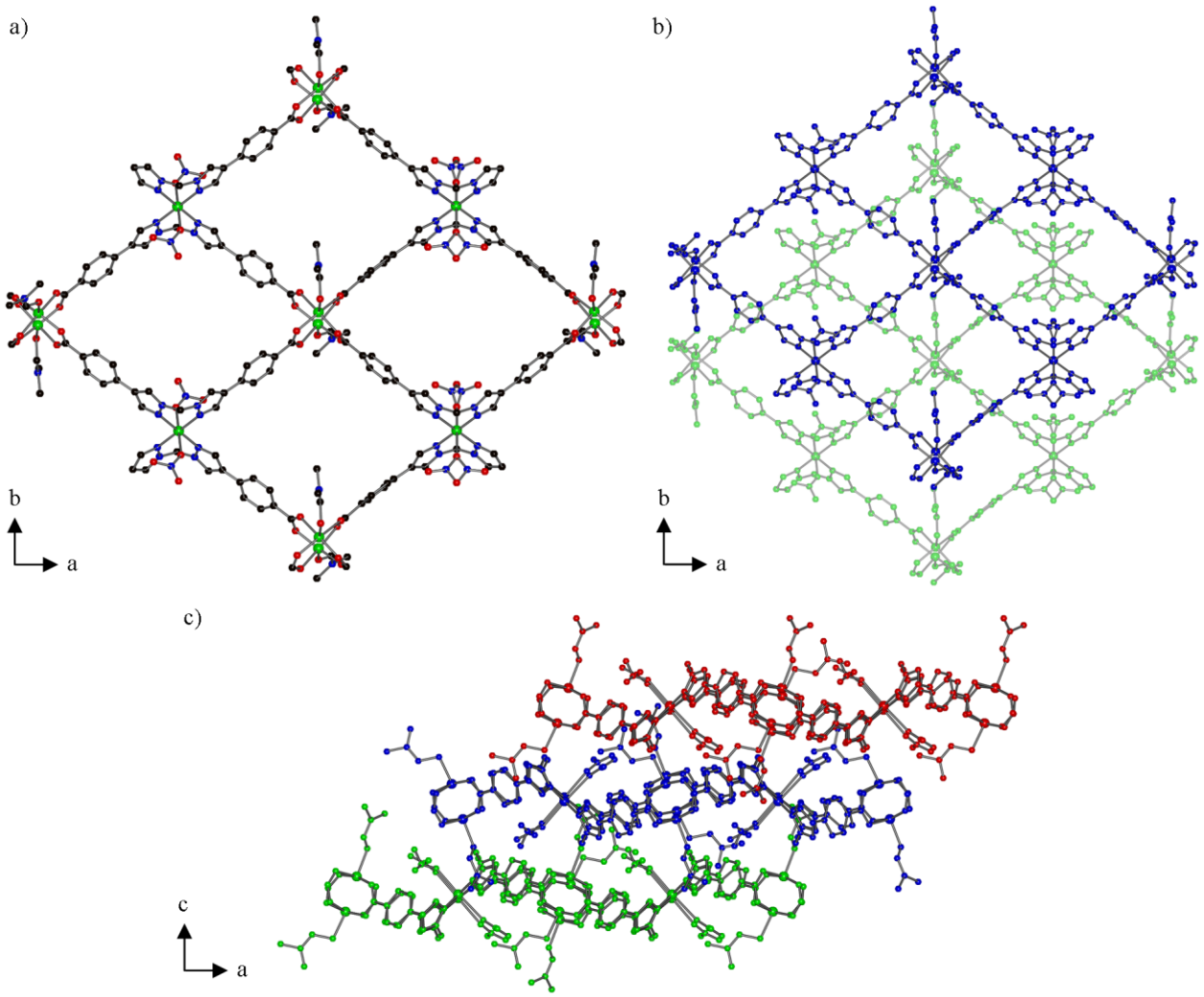

Figure 3.a) A view of the 2-D 4^4net in **1** along the *c*-axis. Views of the staggered 4^4 nets of **1** along b) the *c*-axis and c) the *b*-axis. Hydrogen atoms removed for clarity.

paddlewheel cluster capped by DMF ligands, while the other two copper(II) centres are octahedral and coordinated by two chelating bis-pyrazolylmethane moieties and two monodentate nitrate anions. It is noteworthy that **1** is comprised of two distinct metal nodes yet is synthesised from one type of ligand, albeit one with distinct coordination sites, and a single metal salt. The regular diamond-shaped windows of **1** span *ca.* 15.2 × 19.0 Å between octahedral copper(II) centres and Cu_2 paddlewheel dimers respectively. Close inspection of the structure shows that the 2-D layers of **1** pack in a staggered formation that prevents open channels along the *a*, *b*, and *c* axis (Figures 3b and 3c). The 2-D layers of **1** are held in position by van der Waals interactions that occur between a coordinated DMF solvate molecule and a carbon (phenyl ring) of **bcppm**, with a distance of 2.871Å.

Interestingly, co-planarity of pyrazole and phenyl rings for **bcppm** is observed in the 2-D structure of **1**. In order to explore the topological transformation that would result from perturbing this structural feature, we synthesised the tetramethyl substituted ligand H_2**bcpdmpm** following our established conditions.[22] We hypothesised that the additional steric bulk of the methyl groups would lead to a permanent twist in the backbone of the ligand, and thus promote a different geometrical arrangement. H_2**bcpdmpm** is substantially more soluble than H_2**bcppm** but nonetheless, by modifying the solvothermal reaction conditions for MOF synthesis, reaction of H_2**bcpdmpm** with $Cu(NO_3)_2{\cdot}2½H_2O$ in a mixture of DMF, water, ethanol and 70% HNO_3 at 85°C for 16 hrs gave green rod-like crystals of $\{Cu_4[Cu^I(\mathbf{bcpdmpm})_2]_2(EtOH)_2(H_2O)_2\}(NO_3)_2{\cdot}12DMF$ (**2**) suitable for X-ray crystallography. Due to the structural complexity and low density of the material, synchrotron radiation was required for single crystal and powder diffraction experiments. PXRD confirmed phase purity of the material (Figure 2, bottom).

MOF **2** crystallises in the monoclinic space group $P2_1/c$ with a cell volume of 24480(2) $Å^3$. The structure contains six independent copper atoms in total, four copper(II) centres that constitute two dinuclear paddlewheel units and two tetrahedral copper(I) centres. The latter were considered as Cu(I) centres as a tetrahedral geometry is far more common for d^{10} transition metals and CHN analysis supported the inclusion of only one nitrate

anion per tetrahedral copper centre.[30] Four molecules of ligand **bcpdmpm** complete the coordination requirements of the two copper(II) paddlewheel clusters, while each ligand chelates to a tetrahedral copper(I) centre *via* di-pyrazolyl methane motif (Figure 4a). The coordination of the paddlewheel copper(II) centres are completed by ethanol solvate molecules in the axial positions, but the nitrate counter-anions of the copper(I) centres

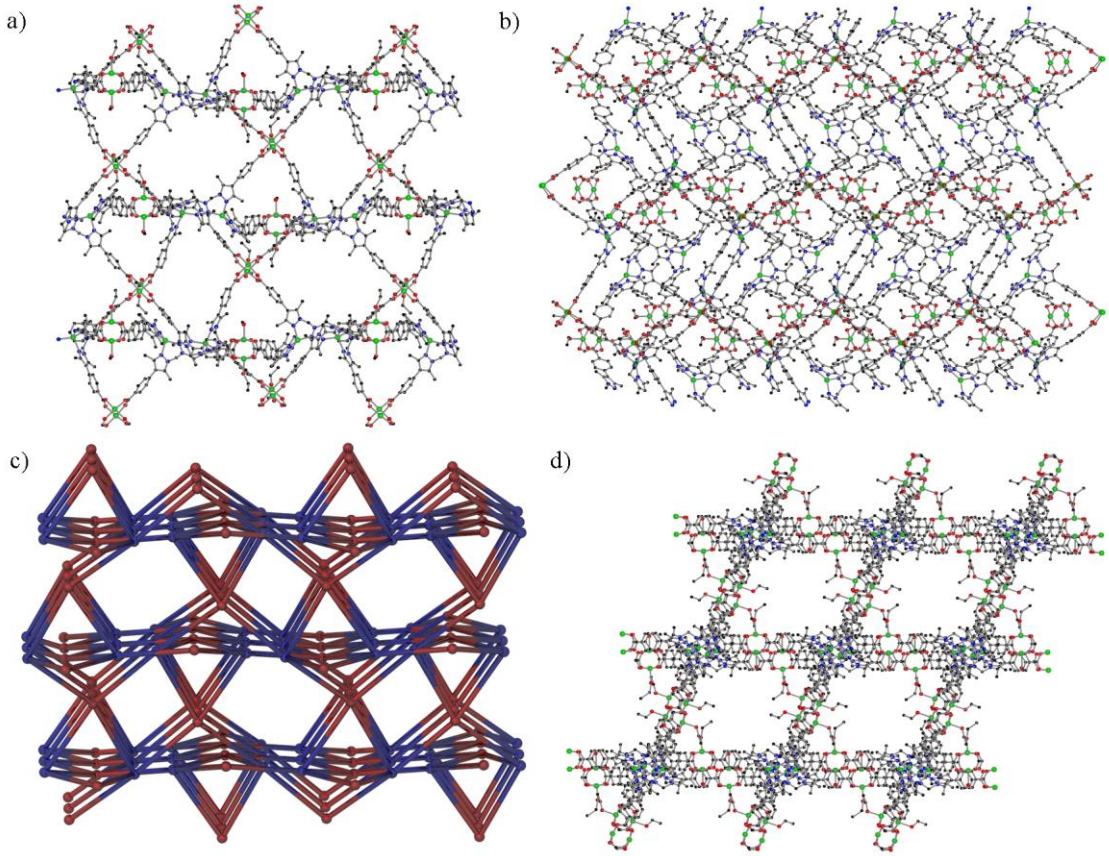

Figure 4.A perspective view of **2** along the a) *a*-axis; b) *c*-axis; and, d) *b*-axis. Hydrogen atoms removed for clarity. c) A topological representation of the tetranodal four-connecting structure, approximately along the *a* axis, with the Cu^{II} paddlewheel nodes in red and tetrahedral Cu^{I} centres shown in blue.

could not be located in the difference map. The coordination chemistry of **bcpdmpm** and the resulting metal nodes are similar to that observed in the 2-D structure of **1**, however the steric influence of the methyl groups in **bcpdmpm** disfavours formation of an octahedral copper(II) and hence an entirely different 3-D MOF structure is obtained.

During synthesis an *in-situ* reduction of copper(II) occurs. Such reductions are not uncommon in the solvothermal synthesis of coordination polymers and have been observed with ligands such as 2,2'-bipyridine (**bpy**) and di-2-pyridylamine.[31-33] Methanol or ethanol can be responsible for the reduction of copper(II) under solvothermal conditions,[34, 35] although the identity of the reducing agent can be unclear.[36] Furthermore, in some cases formation of the copper(I) assembly is reliant on the associated redox mediated modification of the ligand.[37, 38] Nonetheless, examples of mixed valence Cu(II)/Cu(I) coordination polymers are relatively rare,[39] and a majority of these examples contain CN^- or SCN^- co-ligands.[40, 41] Based on literature precedent and the yield of the reaction (63%), the identity of the reducing agent is likely to be ethanol. The *in-situ* reduction is further supported by the angles about the tetrahedral copper centres of **2** which compare favourably to the bond angles of a known Cu(I) complex $[Cu(\mathbf{bpy})_2]ClO_4$[42] (Table SI 1).

The paddlewheel and tetrahedral copper centres both serve as four connecting nodes, leading to a self-interpenetrated tetranodal 4-connected 3-D structure (Figure 4). Self interpenetration is known though not commonly observed among MOF materials,[43, 44] and no reports exists of such materials being permanently porous. MOF **2** has a very low calculated density (0.890 cm^3/g for the solvated material, ~0.6 cm^3/g desolvated) and possesses distinct pores which can be seen along the *a* and *b* axes, while the *c* axis of the structure is essentially close-packed (Figure 4). Interestingly, a high density of copper(II) paddlewheels line the border of the rhombus-shaped pores along the *b*-axis (Figure 4d). Taking into account the van der Waals radii of surrounding atoms and excluding the solvates coordinated to the paddlewheels, the pores along the *b*-axis measure 7.8 × 11.6 Å. Using the same methodology, the three distinct pores along the *a*-axis measure 3.6 × 3.9 Å, 5.0 × 8.8 Å, and 5.8 × 15.6 Å.

Post-synthetic structural changes and gas adsorption properties

A desolvated form of **1** ($\{Cu_2[Cu^{II}(NO_3)_2(\mathbf{bcppm})_2]\}$, $\mathbf{1^{ac}}$) was prepared by heating a dichloromethane (DCM) exchanged sample at 50°C overnight under high vacuum (Figure 2, top). Thermogravimetric analysis (TGA) of $\mathbf{1^{ac}}$ showed a gradual loss

of 8.0% up to 250°C, at which point the steep drop in weight indicated decomposition of the material (Figure SI 2). The ^{1}H NMR spectrum of a digested sample of **1^{ac}** did not show any chemical shifts due to solvent molecules (DMF, MeOH, DCM), while CHN analysis suggested the formulation $\{Cu_2[Cu^{II}(NO_3)_2(\mathbf{bcppm})_2](H_2O)_2\}\cdot H_2O$. This is consistent with observations made when exposing activated samples to ambient conditions which resulted in an immediate colour change from olive green to light green, indicating coordination of the paddlewheel dimers by water molecules. Absorption of moisture by activated MOFs is commonly observed in the literature, especially in MOF materials composed of copper(II) paddlewheels.[45]

The PXRD of as-synthesised **1** was in good agreement with that simulated from the crystal structure, however the activated sample, **1^{ac}**, showed subtle shifts for the higher angle data, indicating a minor structural adjustment (Figure 2, top). As previously mentioned, the shortest contact between the 2-D layers arises from a van der Waals interaction between an apically coordinated DMF ligand and a molecule of **bcppm** from an adjacent layer and thus the structural change is likely to result from the loss of the DMF ligands from the copper(II) paddlewheel. Re-examination of the crystal structure of **1** with the paddlewheel solvent molecules removed reveals a channel along the 202 plane of the structure (Figure SI 1). These 1-D pores measure approximately 4.0 x 6.5 Å, which indicates that the desolvated material should adsorb both N_2 and CO_2, potentially with a high affinity for CO_2 due to channels lined with unsaturated copper(II) metal sites.

A 77 K N_2 isotherm performed in **1^{ac}** revealed a marginal gas uptake of (3.2 cm^3/g at P/P_o = 0.94), while adsorption of CO_2 at 195K gave a type I isotherm with a maximum uptake of 32.5 cm^3/g at P/P_o = 0.95 (Figure SI 3). The BET and Langmuir surface areas were calculated from the 195 K CO_2 isotherm using the criteria detailed by Walton and Snurr,[46] giving values of 75.3 ± 0.9m^2/g and 110.0 ± 1.8 m^2/g respectively. A noticeable hysteresis supports the presence of narrow channels in the structure of **1^{ac}**. At both 293 and 273 K, CO_2 isotherms show a steep uptake at low pressures and total uptakes of 1.0 mmol (22.7 cm^3/g) and 1.2 mmol (26.8 cm^3/g) at 1200 mbar respectively. This isotherm profile and uptake is consistent with a combination of unsaturated Cu^{2+} sites and a small pore volume (Figure 5).[47, 48] It is worth noting that high surface area copper(II) MOFs with exposed Cu^{2+} centres such as Cu-BTC,[49] Cu-BTTri,[50] and NU-100[45] typically exhibit linear uptake of CO_2 at 298 K. This suggests that the ratio of internal pore volume to density of exposed metal sites is important for enhanced low pressure CO_2 adsorption. At 273 K, an expected linear uptake of N_2 was observed, amounting to 0.13 mmol (3.0 cm^3/g) at 1200 mbar (Figure 5). The low N_2 uptake in the 77 and 273 K and negligible uptake 293 K suggests that the pore size of **1**^{ac} may be close to the kinetic diameter of N_2.

The enthalpy of adsorption was calculated for **1^{ac}**, using the virial method,[51] and afforded a value of -35.3 kJ/mol at low coverage (-36.1 kJ/mol using the Clausius-Clapeyron equation,[52] Figure SI 4). This is in the lower range of enthalpy values for MOFs with open metal sites, which typically range from -21 to-62 kJ/mol for CO_2.[53, 54] However, the enthalpy is slightly higher than other MOFs with exposed copper(II) paddlewheels such as HKUST-1 (-30 kJ/mol)[55] and CuBTTri (-21 kJ/mol).[50] Due to the relatively low surface area of **1^{ac}**, the uptake capacity at room temperature (1.1 mmol/g) is significantly lower than that of HKUST-1 and CuBTTri, which have a maximum uptake of 4.7 mmol and 3.8 mmol at 1200 mbar and 1100 mbar respectively. We also note that narrow limiting pore diameters can contribute to CO_2 affinity.[22, 56, 57]

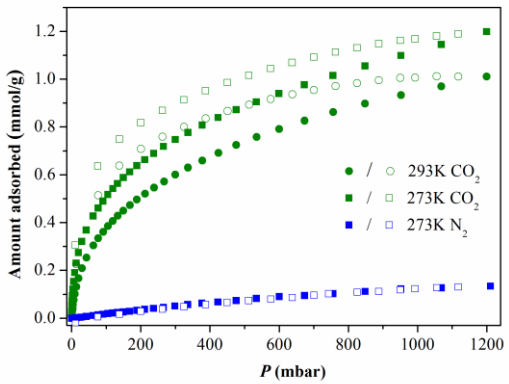

Figure 5. CO_2 and N_2 isotherms for **1^{ac}**.

Structural studies and TGA of **2** indicated that the material was potentially highly porous; thus experiments were carried out to access an activated form for gas adsorption studies. TGA experiments revealed a 63.9% weight loss due to solvent up to 130°C and that the material was thermally stable up 260°C (Figure SI 5). Again, solvent exchange resulted in colour changes that were consistent with exchange of ligands at the axial coordination sites of the copper(II) paddlewheels. Heating a DCM exchanged sample at 50°C for 16 hrs gave the activated sample $[Cu_4[Cu^I(\mathbf{bcpdmpm})_2]_2\}(NO_3)_2$ (**2^{ac}**) which was accompanied by a colour change of the crystals from blue to a light green colour. Desolvation was confirmed by a TGA trace of **2^{ac}** which showed a minimal weight loss of 2.7%.

Again, while phase purity of as-synthesised **2** had been confirmed, PXRD of **2^{ac}** indicated a significant structural change (Figure 2, bottom). The data showed a shift of the low angle Miller indices and a complete absence of higher angle diffraction indicating that a significant structural change occurs during desolvation. Initial gas adsorption measurements for **2^{ac}** revealed that the material was essentially non-porous to N_2. CO_2 uptake at 195 K gave a type I isotherm with a maximum uptake of 44.2 cm^3/g at P/Po = 0.99 (Figure SI 6). Based on the CO_2 isotherm the BET and Langmuir surface areas were estimated to be 149.3 ± 0.7 m^2/g and 198.7 ± 0.9 m^2/g, respectively. These values are well below the calculated geometric surface area (~3000 m^2/g) and, along with PXRD data, suggest that a structural collapse occurred on activation. Other methods of activation were attempted, such as supercritical CO_2 activation and freeze drying,[58-60] however these were unfruitful. Furthermore, resolvation of the activated material with various solvents did not regenerate the original structure indicating an irreversible structural transformation. To further elucidate the structural change, CO_2 isotherms at 273 and 293 K were recorded (Figure SI 7). Both revealed a near linear uptake, which combined with

the low surface area of **2^{ac}**, suggests the absence of accessible unsaturated metal sites due to the structural transformation.

Conclusions

Here we have reported an extension of our approach for generating MOFs with restricted flexibility by describing two new copper-containing MOF materials that utilise a flexible 'hinged' bis-pyrazolylmethane ligand. With **bcppm** a 2-D layered MOF was obtained that upon activation yielded a permanently porous material. In contrast, a 3-D MOF was isolated from reactions of **bcpdmpm** and $Cu(NO_3)_2{\cdot}2½H_2O$. X-ray crystallography of **2** revealed a self-interpenetrated structure composed of Cu(II) paddlewheels and tetrahedral Cu(I) centres coordinated by the distinct donor sets within **bcpdmpm**. Despite possessing large solvent accessible pores along the *a* and *b* axis, desolvation of the material yielded a relatively non porous form, with a notably different structure. MOF **1** showed a favourable adsorption for CO_2 over N_2 at room temperature which was rationalised by the relatively small pore diameter and the presence of unsaturated Cu^{2+} metal sites.

Both reported materials display different extents of structural flexibility in the solid-state and lie in different places on the classification continuum for flexible materials described by Kitagawa. MOF **1** undergoes slight structural changes upon desolvation but is probably best described as a 2nd generation material, while MOF **2** is perhaps better considered as a 1st generation material (non-recoverable structural collapse) despite showing some porosity following its structural change. As shown in our previous and current work, the implementation of a methylene 'hinge' backbone impacts favourably on structural flexibility in MOF materials, however, this work also highlights that the flexibility is governed by the need for alterations in the coordination geometry around the metal ion coordinated by the 'hinge' donors. Importantly, this study also demonstrates that this class of hinged ligands can form metal nodes exclusively from one type of donor, giving rise MOF materials containing two distinct structural nodes. We are continuing to explore examples of this fascinating group of materials with respect to their gas adsorption properties.

Acknowledgements

CJD and CJS gratefully acknowledge the Australian Research Council for funding (FT100100400 and FT0991910). We also acknowledge the Science and Industry Endowment Fund for financial support. Aspects of this research were undertaken on the Powder Diffraction beamline at the Australian Synchrotron, Victoria, Australia. Prof. M O'Keeffe is thanked for helpful discussions on the topology of **2**.

Notes and references

[a] *School of Chemistry and Physics, The University of Adelaide, SA 5005, Australia. Phone +61 8 8313 7406. Fax. +61 8 8313 4358. Email:* christopher.sumby@adelaide.edu.au

† Electronic Supplementary Information (ESI) available: alternative views of structure **1**, bond angles for the Cu^{I} centres in **2**, thermogravimetric analysis data, gas adsorption isotherms for **1** and **2**, and enthalpy of adsorption data. See DOI: 10.1039/b000000x/

1. S. Kitagawa, R. Kitaura and S.-I. Noro, *Angew. Chem. Int. Ed.*, 2004, **43**, 2334-2375.
2. S. Kitagawa and K. Uemura, *Chem. Soc. Rev.*, 2005, **34**, 109-119.
3. S. Horike, S. Shimomura and S. Kitagawa, *Nat. Chem.*, 2009, **1**, 695-704.
4. G. Ferey and C. Serre, *Chem. Soc. Rev.*, 2009, **38**, 1380-1399.
5. C. Serre, F. Millange, C. Thouvenot, M. Noguès, G. Marsolier, D. Louër and G. Férey, *J. Am. Chem. Soc.*, 2002, **124**, 13519-13526.
6. K. Uemura, R. Matsuda and S. Kitagawa, *J. Solid State Chem.*, 2005, **178**, 2420-2429.
7. J.-P. Zhang, S. Horike and S. Kitagawa, *Angew. Chem. Int. Ed.*, 2007, **46**, 889-892.
8. S. Shimomura, M. Higuchi, R. Matsuda, K. Yoneda, Y. Hijikata, Y. Kubota, Y. Mita, J. Kim, M. Takata and S. Kitagawa, *Nat. Chem.*, 2010, **2**, 633-637.
9. J.-R. Li, R. J. Kuppler and H.-C. Zhou, *Chem. Soc. Rev.*, 2009, **38**, 1477-1504.
10. D. Tanaka, K. Nakagawa, M. Higuchi, S. Horike, Y. Kubota, T. C. Kobayashi, M. Takata and S. Kitagawa, *Angew. Chem. Int. Ed.*, 2008, **47**, 3914-3918.
11. H.-S. Choi and M. P. Suh, *Angew. Chem. Int. Ed.*, 2009, **48**, 6865-6869.
12. P.-Q. Liao, D.-D. Zhou, A.-X. Zhu, L. Jiang, R.-B. Lin, J.-P. Zhang and X.-M. Chen, *J. Am. Chem. Soc.*, 2012, **134**, 17380-17383.
13. T. K. Kim and M. P. Suh, *Chem. Commun.*, 2011, **47**, 4258-4260.
14. P. Kanoo, R. Sambhu and T. K. Maji, *Inorg. Chem.*, 2010, **50**, 400-402.
15. D. N. Dybtsev, H. Chun and K. Kim, *Angew. Chem. Int. Ed.*, 2004, **43**, 5033-5036.
16. N. Yanai, K. Kitayama, Y. Hijikata, H. Sato, R. Matsuda, Y. Kubota, M. Takata, M. Mizuno, T. Uemura and S. Kitagawa, *Nat. Mater.*, 2011, **10**, 787-793.
17. P. Horcajada, T. Chalati, C. Serre, B. Gillet, C. Sebrie, T. Baati, J. F. Eubank, D. Heurtaux, P. Clayette, C. Kreuz, J.-S. Chang, Y. K. Hwang, V. Marsaud, P.-N. Bories, L. Cynober, S. Gil, G. Ferey, P. Couvreur and R. Gref, *Nat. Mater.*, 2010, **9**, 172-178.
18. P. Horcajada, C. Serre, G. Maurin, N. A. Ramsahye, F. Balas, M. a. Vallet-Regí, M. Sebban, F. Taulelle and G. Férey, *J. Am. Chem. Soc.*, 2008, **130**, 6774-6780.
19. C. Serre, C. Mellot-Draznieks, S. Surblé, N. Audebrand, Y. Filinchuk and G. Férey, *Science*, 2007, **315**, 1828-1831.
20. H. J. Park and M. P. Suh, *Chem. Commun.*, 2010, **46**, 610-612.
21. W. M. Bloch and C. J. Sumby, *Chem. Commun.*, 2012, **48**, 2534-2536.
22. W. M. Bloch, R. Babarao, M. R. Hill, C. J. Doonan and C. J. Sumby, *J. Am. Chem. Soc.*, 2013, DOI: 10.1021/ja4032049.
23. M. Du, X.-G. Wang, Z.-H. Zhang, L.-F. Tang and X.-J. Zhao, *CrystEngComm*, 2006, **8**, 788-793.
24. M. Du, Z.-H. Zhang, X.-G. Wang, L.-F. Tang and X.-J. Zhao, *CrystEngComm*, 2008, **10**, 1855-1865.
25. A. S. Potapov, A. I. Khlebnikov and S. F. Valisevskii, *Russ. J. Org. Chem.*, 2006, **42**, 1368-1373.
26. G. M. Sheldrick, *Acta Crystallog., Section A*, 1990, **46**, 467-473.
27. G. M. Sheldrick, SHELXL-97, University of Göttingen, Göttingen, Germany, 1997.
28. L. J. Barbour, *J. Supramol. Chem.*, 2001, **1**, 189-191.
29. A. L. Spek, *Acta Crystallog., Section A*, 1990, **46**, C34.
30. J. Cirera, P. Alemany and S. Alvarez, *Chem., Eur. J.*, 2004, **10**, 190-207.
31. J. Y. Lu, B. R. Cabrera, R.-J. Wang and J. Li, *Inorg. Chem.*, 1998, **37**, 4480-4481.
32. J. Y. Lu, B. R. Cabrera, R.-J. Wang and J. Li, *Inorg. Chem.*, 1999, **38**, 4608-4611.
33. O. M. Yaghi and H. Li, *J. Am. Chem. Soc.*, 1995, **117**, 10401-10402.
34. S. M. F. Lo, S. S. Y. Chui, L.-Y. Shek, Z. Lin, X. X. Zhang, G.-H. Wen and I. D. Williams, *J. Am. Chem. Soc.*, 2000, **122**, 6293-6294.
35. S. Banthia and A. Samanta, *Inorg. Chem.*, 2004, **43**, 6890-6892.
36. J. Y. Lu, *Coord. Chem. Rev.*, 2003, **246**, 327-347.
37. A. Banisafar and R. L. LaDuca, *Inorg. Chim. Acta*, 2011, **373**, 295-300.

38. G.-P. Yong, Y.-M. Zhang and B. Zhang, *CrystEngComm*, 2012, **14**, 8620-8625.
39. H. Zhao, Z.-R. Qu, Q. Ye, X.-S. Wang, J. Zhang, R.-G. Xiong and X.-Z. You, *Inorg. Chem.*, 2004, **43**, 1813-1815.
40. D. Sadhukhan, C. Rizzoli, E. Garribba, C. J. Gomez-Garcia, A. Yahia-Ammar, L. J. Charbonniere and S. Mitra, *Dalton Trans.*, 2012, **41**, 11565-11568.
41. F. Xu, T. Tao, K. Zhang, X.-X. Wang, W. Huang and X.-Z. You, *Dalton Trans.*, 2013, **42**, 3631-3645.
42. M. Munakata, S. Kitagawa, A. Asahara and H. Masuda, *Bull. Chem. Soc. Jpn*, 1987, **60**, 1927-1929.
43. S.-Y. Wan, Y.-T. Huang, Y.-Z. Li and W.-Y. Sun, *Micropor. Mesopor. Mat.*, 2004, **73**, 101-108.
44. J. Yang, B. Li, J.-F. Ma, Y.-Y. Liu and J.-P. Zhang, *Chem. Commun.*, 2010, **46**, 8383-8385.
45. O. K. Farha, A. Özgür Yazaydın, I. Eryazici, C. D. Malliakas, B. G. Hauser, M. G. Kanatzidis, S. T. Nguyen, R. Q. Snurr and J. T. Hupp, *Nat. Chem.*, 2010, **2**, 944-948.
46. K. S. Walton and R. Q. Snurr, *J. Am. Chem. Soc.*, 2007, **129**, 8552-8556.
47. P. D. C. Dietzel, V. Besikiotis and R. Blom, *J. Mater. Chem.*, 2009, **19**, 7362-7370.
48. S. R. Caskey, A. G. Wong-Foy and A. J. Matzger, *J. Am. Chem. Soc.*, 2008, **130**, 10870-10871.
49. P. Aprea, D. Caputo, N. Gargiulo, F. Iucolano and F. Pepe, *J. Chem. Eng. Data*, 2010, **55**, 3655-3661.
50. A. Demessence, D. M. D'Alessandro, M. L. Foo and J. R. Long, *J. Am. Chem. Soc.*, 2009, **131**, 8784-8786.
51. T. M. McDonald, D. M. D'Alessandro, R. Krishna and J. R. Long, *Chem. Sci.*, 2011, **2**, 2022-2028.
52. L. Czepirski and J. Jagiello, *Chem. Eng. Sci.*, 1989, **44**, 797-801
53. K. Sumida, D. L. Rogow, J. A. Mason, T. M. McDonald, E. D. Bloch, Z. R. Herm, T.-H. Bae and J. R. Long, *Chem. Rev.*, 2012, **112**, 724-781.
54. C. R. Wade and M. Dinca, *Dalton Trans.*, 2012, **41**, 7931-7938.
55. Q. Min Wang, D. Shen, M. Bülow, M. Ling Lau, S. Deng, F. R. Fitch, N. O. Lemcoff and J. Semanscin, *Micropor. Mesopor. Mat.*, 2002, **55**, 217-230.
56. P. Nugent, Y. Belmabkhout, S. D. Burd, A. J. Cairns, R. Luebke, K. Forrest, T. Pham, S. Ma, B. Space, L. Wojtas, M. Eddaoudi and M. J. Zaworotko, *Nature*, 2013, **495**, 80-84.
57. M. Wriedt, J. P. Sculley, A. A. Yakovenko, Y. Ma, G. J. Halder, P. B. Balbuena and H.-C. Zhou, *Angew. Chem. Int. Ed.*, 2012, **51**, 9804-9808.
58. A. P. Nelson, O. K. Farha, K. L. Mulfort and J. T. Hupp, *J. Am. Chem. Soc.*, 2008, **131**, 458-460.
59. O. K. Farha and J. T. Hupp, *Acc. Chem. Res.*, 2010, **43**, 1166-1175.
60. L. Ma, A. Jin, Z. Xie and W. Lin, *Angew. Chem. Int. Ed.*, 2009, **48**, 9905-9908.

